

## Chirped Pulse Amplification

Jeff Squier, Charles Durrfee III, Thomas Planchon  
Department of Physics, Colorado School of Mines, USA

G rard Mourou  
ENSTA, France

### I. Introduction

Over the past twenty years we have seen a spectacular increase in laser peak power and, consequently, focused laser intensity. The key to achieving these ultrahigh peak powers has been the successful amplification of picosecond and femtosecond laser pulses (Figure 1). Since the first laser demonstration in 1960, the laser pulse duration has continuously decreased from the range of microseconds with the free running laser, to nanoseconds with the advent of Q-switching, and finally to the picosecond and few femtosecond regime with the introduction of mode-locking.

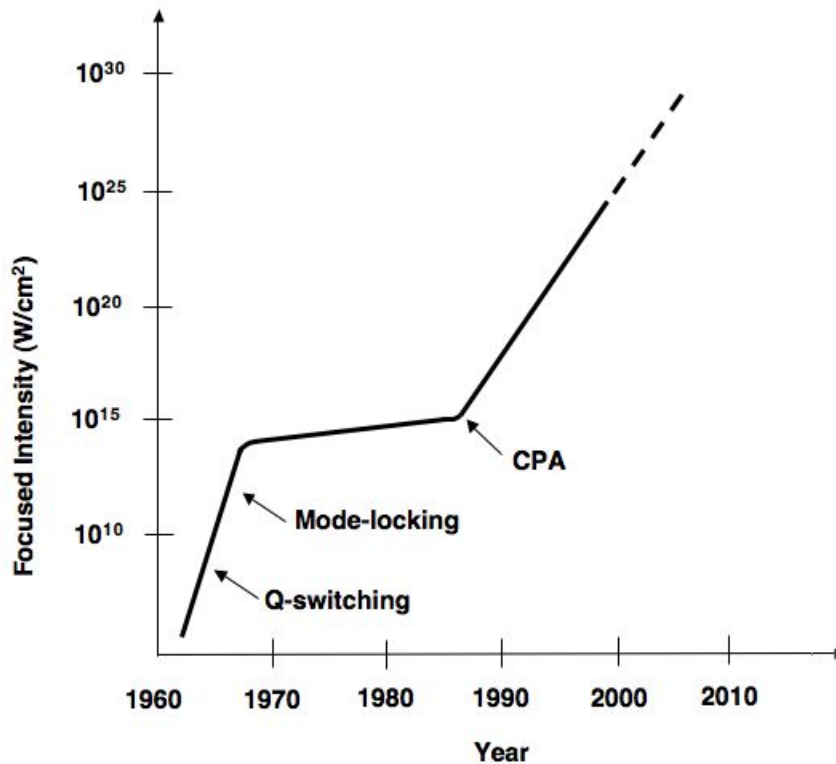


Figure 1 : Laser intensity versus years. Note the very steep slope in intensities that occurs during the 60's. This period corresponded to the discovery of most nonlinear optics effects due to the bound electron. Today, we are experiencing a similar rapid increase in intensity opening a new regime in optics dominated by the relativistic character of the electron.

However, with mode-locking, new challenges were created. The laser pulse duration became so short that the pulses could not be amplified directly without

producing unwanted nonlinear effects. Consequently, the laser peak power and intensity effectively plateaued by the mid 1960's (Figure 1). For reasonable size systems, (i.e., systems with beam diameters on the order of 1 cm) the maximum obtainable peak power hovered near 1GW, limiting focused intensities to approximately  $10^{14}\text{W/cm}^2$  for the next twenty years.

If laboratory scale lasers were to escape the peak power plateau, at least two more ingredients were necessary. One, amplifiers had to incorporate gain media with bandwidth sufficient to support the amplification of the picosecond and femtosecond pulses that oscillators were suddenly capable of producing. Two, to maintain a reasonable spatial scale, these same gain media would need to be capable of high-energy storage.

Gain media with these characteristics were quickly identified. However, it came at a cost – materials with these characteristics have a small stimulated emission cross section,  $\sigma_{21}$ . As we will see later in the chapter, efficient energy extraction demands that the input laser fluence -to the amplifier- be of the order of the saturation fluence

$$F_{sat} = \hbar\omega / \sigma_{21} \quad (1)$$

where  $\hbar$  is Planck's constant,  $\omega$  is the central laser frequency, and  $\sigma_{21}(\omega)$  is the stimulated emission cross section at the laser wavelength.

Thus, a small cross section,  $\sigma_{21}$ , necessarily results in a large saturation fluence. For solid-state laser materials this energy fluence ranges from 1 to 20 J/cm<sup>2</sup>. If we are amplifying an ultrashort pulse at these fluences, the intensity at any given moment is found by dividing the saturation fluence by the laser pulse duration. For instance, if we are to amplify a 100 fs pulse in a media within the cited saturation fluence range, the resulting intensity in the amplifier chain will be on the order of 10 to 200 TW/cm<sup>2</sup>. This is well above the  $\sim \text{GW/cm}^2$  limit imposed by nonlinear effects and optical damage in typical amplifiers and optical components!

Consequently gain media with these characteristics couldn't be employed, and the only alternative was to use low saturation fluence, low energy storage materials (dyes and excimers) and increase the laser beam cross section (scaling the beam aperture size lowers the intensity). This subsequently led to unattractive, large, low repetition rate, high-price tag systems. High intensity laser physics was therefore relegated to the realm of the national labs, and had to be performed on a limited number of laser systems, such as the CO<sub>2</sub> laser found at Los Alamos National Laboratory<sup>1</sup>, or the Nd: glass at the Laboratory for Laser Energetics<sup>2</sup> and excimer lasers at the University of Illinois at Chicago and the University of Tokyo<sup>3,4</sup>.

- **Breaking the Energy-Pulse Duration Quadrature**

The state of affairs changed dramatically in 1985 when laser physicists at the University of Rochester<sup>5-7</sup> demonstrated a way to circumvent what seemed to be an intractable problem: efficient energy extraction from a broad bandwidth, high saturation fluence, solid-state laser media, by an ultrashort laser pulse. The solution was a technique, that was coined CPA by the inventors, and stood for **Chirped Pulse Amplification**.

It revolutionized the field in at least three major ways. First, *table-top* laser systems incorporating CPA became capable of delivering intensities  $10^5$ - $10^6$  times higher

than in the past. Second, the CPA technique could be readily adapted to existing large laser fusion systems at a relatively low cost. (In fact, today CPA is incorporated into virtually all the major laser facilities, in Japan<sup>8</sup>, France<sup>9</sup>, the United Kingdom, the United-States<sup>10</sup>, etc. The main application at these large national facilities is Fast Ignition research<sup>11</sup>.) Third, because of their reduced size, CPA lasers could be installed near large particle accelerators such as synchrotrons<sup>12,13</sup> or near linear colliders such as SLAC to produce fields higher than the critical field<sup>14</sup> to observe nonlinear QED effects like pair generation from vacuum. At the moment, colliders world-wide are considering the incorporation of CPA technology to produce  $\gamma$ -rays for photon-photon scattering, i.e. the  $\gamma$ - $\gamma$  collider<sup>15-18</sup>.

As we describe in the book, the availability of these ultrahigh intensity lasers has extended the horizon of laser physics from atomic and condensed phase physics to plasma physics, nuclear physics, high-energy physics, general relativity and cosmology. CPA also had a major effect in bringing back to the university laboratory, science that was previously only performed on large, national laboratory scale instruments.

- **Short Pulse Amplification - Propagation condition**

As the laser pulse is amplified it must necessarily propagate through the amplifier medium without experiencing wavefront distortion. Prior to CPA the amplifying media were exclusively, dyes<sup>19</sup>, or excimers<sup>3,4</sup>. Typical cross-section for these media is very large - in the range of  $10^{-16} \text{cm}^2$  -implying a saturation fluence  $F_{sat}$  of only few  $\text{mJ}/\text{cm}^2$  or a power density of  $1\text{GW}/\text{cm}^2$  for subpicosecond pulses. Above this power density level, the index of refraction  $n$  becomes intensity dependent according to the well-known expression

$$n(x,t) = n_0 + n_2 I(x,t) \quad (2)$$

where  $n_0$  is the index of refraction at low intensity and  $I(x,t)$  the laser intensity. Due to the spatial variation of the laser beam intensity this will modify the beam wave-front according to

$$B(t) = \frac{2\pi n_0}{\lambda} \int_0^L n_2 I(x,t) dx \quad (3)$$

Here,  $\lambda$  is the laser wavelength.  $B$  represents in  $\lambda$ , the amount of wavefront distortion accumulated by the beam over a length  $L$ . For a perfectly Gaussian beam,  $B$  will cause the whole beam to self-focus above a critical power given by the expression

$$P_{cr} = \frac{\lambda^2}{2\pi n_0 n_2} \quad (4)$$

The nonlinear index  $n_2$  is typically on the order of  $5 \cdot 10^{-16} \text{cm}^2/\text{W}$ . Note that this effect is strictly power dependent. After a propagation of few centimeters, the wavefront has been altered by a fraction of a wavelength. In the case where the laser beam exhibits some small scale spatial intensity modulation,  $n_2$  will cause the beam to break up in filaments. In practice the small scale self-focusing represents the most severe problem in an amplifier system.

For laser fusion systems, the beam is cleaned through spatial filters, every time  $B$  reaches 3. For high field experiments where the spatial and temporal beam quality is more critical,  $B$  must be kept below 0.3 corresponding to a wavefront distortion of  $\lambda/20$ .

- **The Chirped Pulse Amplification Concept**

Amplification media with low cross-sections offers the tremendous benefit of making the laser extremely compact. For instance, Nd:glass has a cross section of  $10^{-21}\text{cm}^2$  which means that we can store a thousand to ten thousand times more atoms per unit volume and consequently get a thousand to ten thousand times more energy before it self-oscillates. ( Compare this to dyes or excimers with cross-sections on the order of  $\sim 10^{-16}\text{cm}^2$ . ) However, as we have discussed, to extract this energy requires a beam with a fluence  $F_{sat}$  of the order of  $1\text{J}/\text{cm}^2$  or an intensity of  $10^{12}\text{W}/\text{cm}^2$ . This corresponds to a  $B$ -integral of few thousand, i.e. a thousand times the limit established in the previous paragraph!

This quandary is solved with CPA. The basic idea behind CPA is simple. The pulse is first stretched by a factor of a thousand to hundred thousands. This step does not change the input pulse fluence (which is pulse width independent), and therefore our energy extraction capability, but it does however, decrease the input intensity by the stretching ratio. Consequently, this keeps the  $B$ -integral to a reasonable level. Once the pulse is amplified from six to twelve orders of magnitude i.e. from the nJ to the millijoule-kilojoule level, the stretched (chirped), energetic pulse is recompressed by the same stretching ratio back to its transform limit. Clearly, the stretcher-compressor system is the key element in a CPA system.

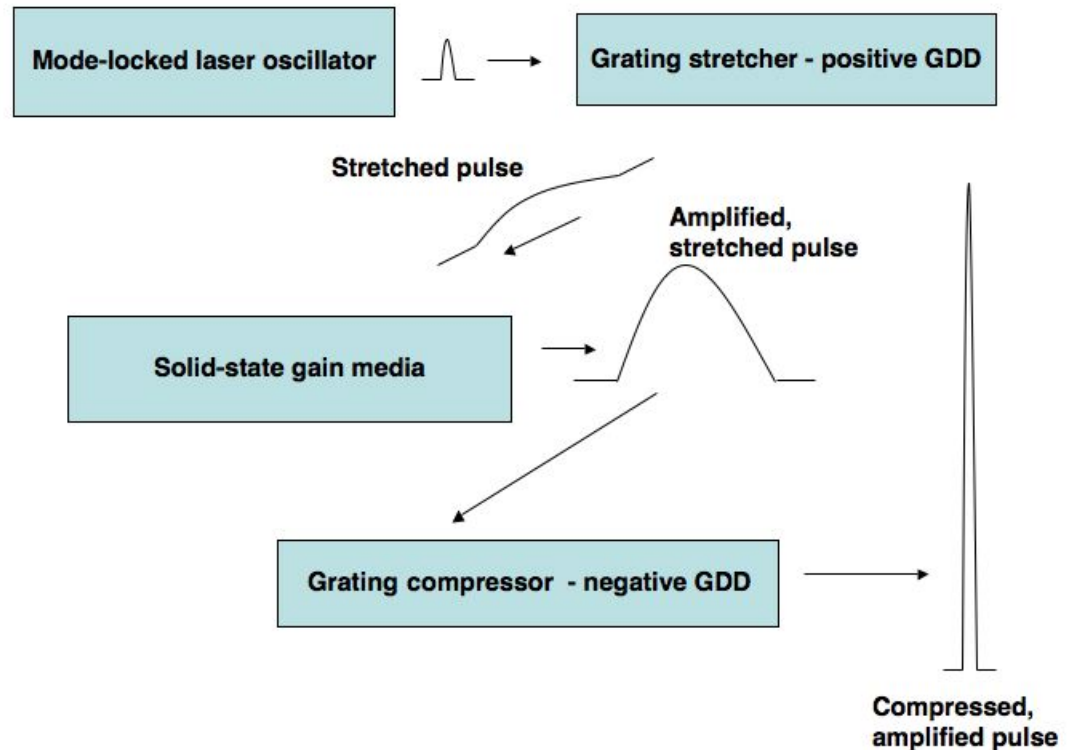


Figure 2 : The chirped pulse amplification concept. To minimize the nonlinear effects the pulse is first stretched several thousand times, lowering the intensity accordingly without changing the input fluence ( $\text{J}/\text{cm}^2$ ). The pulse is then amplified by a factor of  $10^6$  to  $10^{12}$ . The pulse is then compressed to its Fourier transform limit.

- **The Matched Stretcher-Compressor**

In the first CPA embodiment (Strickland and Mourou, 1985<sup>5</sup>) the laser pulse was stretched in an optical fiber (positive group delay dispersion) and compressed by a pair of parallel gratings<sup>20</sup> arranged to provide negative group delay dispersion. Although this first demonstration had led to a spectacular 100 times improvement in peak power, it had the problem that the stretcher and compressor were not perfectly matched – i.e., the dispersion of the compressor (gratings), was not perfectly equal and opposite to the dispersion of the stretcher (a fiber). Unfortunately, after compression the pulse exhibited unacceptable pre-pulses and post-pulses. Therefore, following the first CPA demonstration the Rochester group started to look for the ideal “matched stretcher-compressor system.”

The solution came about when, in 1987, Martinez<sup>21</sup> proposed a grating compressor that could be arranged to provide *positive* group delay dispersion for communication applications. In optical communication applications the wavelength of choice is  $1.5 \mu\text{m}$ , a region where fiber exhibits negative group velocity dispersion. After propagation in a fiber the communication bits exhibit a negative chirp. It is therefore necessary to use a dispersive delay line with a positive group delay dispersion to recompress the pulse.

After examining this device, the Rochester group came to the conclusion that the Martinez “compressor” was in fact the matched stretcher of the Treacy compressor that they had been seeking (this is illustrated later in the chapter).

The phase conjugation of the two systems was demonstrated for the first time by Pessot et al<sup>22</sup> who stretched an 80 fs pulse by a factor of 1000 (to 80 ps) using a Martinez grating pair and compressed it to its original pulse duration (80 fs) using the Treacy compressor. This demonstration represented a major step in Chirped Pulse Amplification. The matched stretcher/compressor concept was incorporated for the first time into a CPA system that was used to produce a Terawatt pulse from a Table Top system -so called T<sup>3</sup>- by the Rochester group. This first system used picosecond pulses, but subpicosecond pulses<sup>6,7</sup> and femtosecond pulse durations<sup>23</sup> quickly followed. This arrangement has become the standard architecture used in almost all CPA systems today (Figure 2).

## II. Design and Construction of a CPA system

- **How far to stretch?**

The basic motivation for chirped pulse amplification should now be clear - we are now set to design a system! The first question we should be asking ourselves then, is how far do we need to stretch (chirp) our input pulse prior to amplification? Unfortunately, there is not a single, simple answer to this question – so to help get started we need to understand a few of the parameters inherent to any laser system to help us make an educated estimate of just how far we will need to stretch our input pulse.

First and foremost we want to avoid damaging our laser – we can use damage thresholds for common coatings found in the laser chain to help with the estimation process. One word of caution here – damage thresholds can vary dramatically from component to component, manufacturer to manufacturer. To further complicate things most optical component/coating companies only quote damage thresholds in terms of 10 ns pulses. A CPA system will generate a chirped pulse in the 10 ps to 1 ns range, so the damage thresholds must be appropriately rescaled. Damage in this range (10 ps to 10 ns) tends to scale as the square root of the pulse width. Thus if a catalog states that the damage threshold of a component is 50 J/cm<sup>2</sup> measured with a 10 ns pulse (500 MW/cm<sup>2</sup>) and we will be using a 100 ps chirped pulse, we can scale the damage threshold accordingly. The ratio of the 10 ns to 100 ps pulse is 100, the square root of this ratio is 10. Thus, for our 100 ps pulse we estimate this optic will have a damage threshold of 5 J/cm<sup>2</sup> (5 GW/cm<sup>2</sup>).

A second important consideration necessary to help us establish an estimate of chirped pulsewidth is extraction efficiency. In general, we will want to extract as much of the energy stored in our amplifier in as efficient a manner as is possible. As stated earlier, laser amplifier efficiency is a strong function of the amplifier saturation fluence given by

$$F_{sat} = \frac{\hbar\omega}{\sigma_{21}} \quad (1)$$

where  $\hbar$  is Planck's constant,  $\omega$  is the central laser frequency, and  $\sigma_{21}(\omega)$  is the stimulated emission cross section at the laser wavelength. For Ti:sapphire at 800 nm the saturation fluence is  $\sim 1.0 \text{ J/cm}^2$ , for Alexandrite at 750 nm wavelength, its  $\sim 20 \text{ J/cm}^2$ . In Figure 3 a plot of extraction efficiency as a function of fluence is generated for Ti:sapphire. What we learn from this type of plot is that to optimize our extraction efficiency we want to operate the amplifier at the saturation fluence of the material. An even more optimal condition - twice the saturation fluence. (Note: this plot and all others in this chapter are generated from the amplifier theory presented by Frantz and Nodvik<sup>24</sup>. These equations are very straight forward to implement and are an outstanding tool for predicting typical amplifier performance. While the equations are reproduced in this chapter, the reader is referred to the original work for a full derivation of these equations.)

We can understand this result physically by looking at our expression for  $F_{\text{sat}}$ . Essentially, it states that if we enter our laser media at the saturation fluence, we are at a density of having a photon per emitter. With this picture in mind, its easy to imagine why the stimulated emission process is most efficient at this density (or higher).

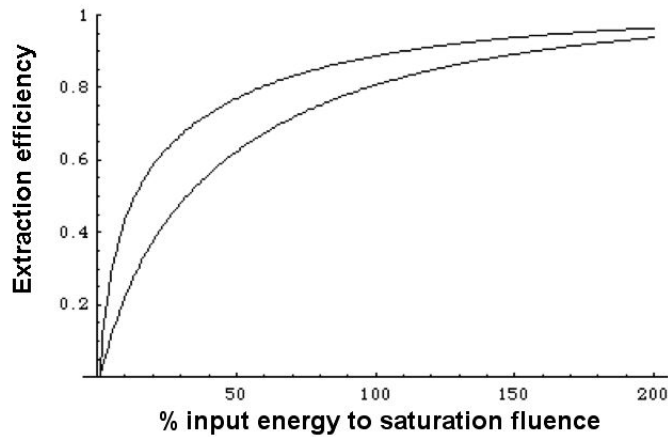


Figure 3 : Extraction efficiency of an amplifier as a function of input fluence. Upper curve – double pass, lower curve, single pass.

We can now put these two quantities together – the saturation fluence establishes an energy fluence we would like to design for to achieve a desired target extraction efficiency. The damage threshold, places an upper bound on the intensity our amplifier can tolerate. These two numbers can be used in conjunction to estimate the chirped pulse duration. Let's use the numbers for Ti:sapphire as an illustration. Assuming a damage threshold of  $5 \text{ GW/cm}^2$  (assuming pulsewidth is  $\sim 100 \text{ ps}$ ), and a desired operating fluence of  $2 \text{ J/cm}^2$ , we estimate needing a chirped pulsewidth on the order of

$$\tau_{\text{chirped}} \sim \frac{1}{I_{\text{damage}}} \cdot \frac{F_{\text{sat}}}{1} = \frac{1}{5 \cdot 10^9} \cdot \frac{2}{1} = 400 \text{ ps} \quad (5)$$

Indeed, examining the literature one finds that the most efficient Ti:sapphire systems are in fact operating at chirped pulse durations in the range from 100 to 400 ps (or greater).

- **Methods of stretching**

Now that we have a means of estimating a target chirped pulsewidth, we can examine the different possibilities for stretching the pulse. In prior chapters the discussion was almost exclusively focused on compensating relatively small amounts of dispersion. By contrast, we now want to purposely induce massive amounts of dispersion, and do so in such a way that it is almost completely (if not entirely) reversible.

In earlier chapters we have seen that there are primarily three methods for producing negative group delay dispersion (GDD): specially designed coatings, prism pairs and grating pairs. Considering only second order dispersion (GDD) the chirped pulse duration,  $\tau_{chirped}$ , is related to the input pulse duration,  $\tau_{initial}$ , by the equation (for a Gaussian pulse)

$$\tau_{chirped} = \tau_{initial} \left( 1 + \left( (4 \ln 2) \left( \frac{GDD}{\tau_{initial}^2} \right) \right)^2 \right)^{0.5} \quad (6)$$

To understand the meaning of this expression, it is useful to make an analogy between the temporal and spatial domains, with the expression describing the evolution of the transverse size of a spatial Gaussian beam as a function of the propagation distance  $z$  :

$$w(z) = w_0 \sqrt{1 + \left( \frac{z}{Z_R} \right)^2} \quad (7)$$

Equation (7) describes the spatial divergence of a Gaussian beam, caused by diffraction, from its waist  $w_0$ . An example of the evolution of pulsewidth, and the spatial beam waist as a function of propagation distance,  $z$ , is shown in Figure 4. We see that the medium dispersion plays the same role in the temporal domain as diffraction does in the spatial domain.

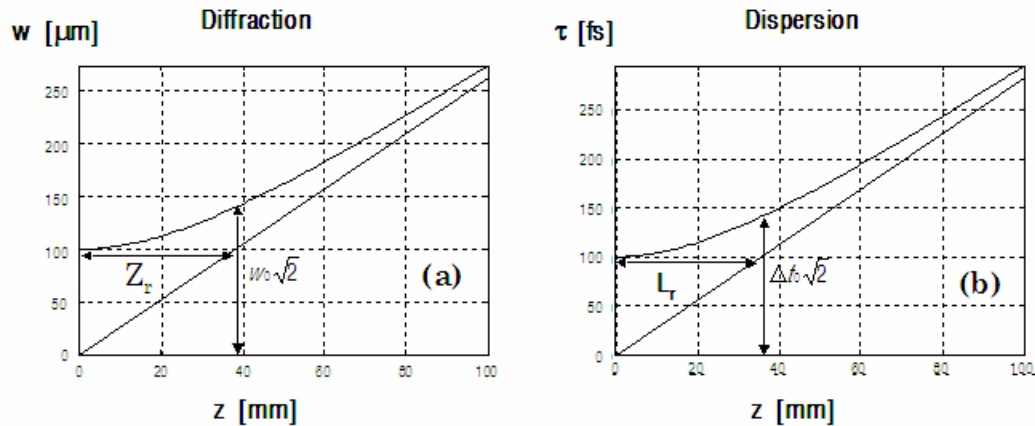


Figure 4 :(a) Spatial evolution of a Gaussian beam for a free-space propagation in air. (b) Temporal evolution of a Gaussian pulse for a propagation in a dispersive medium ( $\omega_0=100$  mm,  $\lambda_c=800$  nm, initial pulsewidth is 100 fs,  $k''(\omega_c)=10^5$  fs<sup>2</sup>.m<sup>-1</sup>)

It is therefore also possible to define a temporal equivalent to the Rayleigh range  $Z_R$  that we can call the “dispersion length”  $L_R$ .

$$L_R = \frac{\tau_{initial}^2}{(4 \ln 2) k''(\omega_c)} \quad (8)$$

This value shows that, the shorter a pulse is initially, the more rapidly it disperses.

Expressions (6 or 8) can be used to estimate the GDD necessary to stretch a pulse from 30 fs to say, 100 ps. At 800 nm, the necessary GDD is  $\sim 1.15 \cdot 10^6$  fs<sup>2</sup>. This is way too much dispersion to be generally practical from coatings, and we can eliminate them from consideration. Prisms are not practical for similar reasons – common glass prisms, spaced by a meter will only generate  $\sim 1000$ - $5000$  fs<sup>2</sup> of GDD. Grating pairs, however, are highly dispersive and can match these magnitudes in a reasonable, compact geometry. For example, a 1200 l/mm grating pair used at an angle-of-incidence of 28.6 degrees requires a separation of only 29.8 cm to produce  $-1.155 \cdot 10^6$  fs<sup>2</sup> of GDD (this is the net double-pass dispersion).

While grating pairs can provide the necessary dispersion, that solves only part of the problem – in a CPA system we need to stretch, amplify and compress. We need two systems capable of large amounts of dispersion – one used to stretch the pulse prior to amplification, the second to compress the pulse post-amplification. In addition these systems must be opposite in sign – positive GDD provided by one system, negative GDD provided by the other.

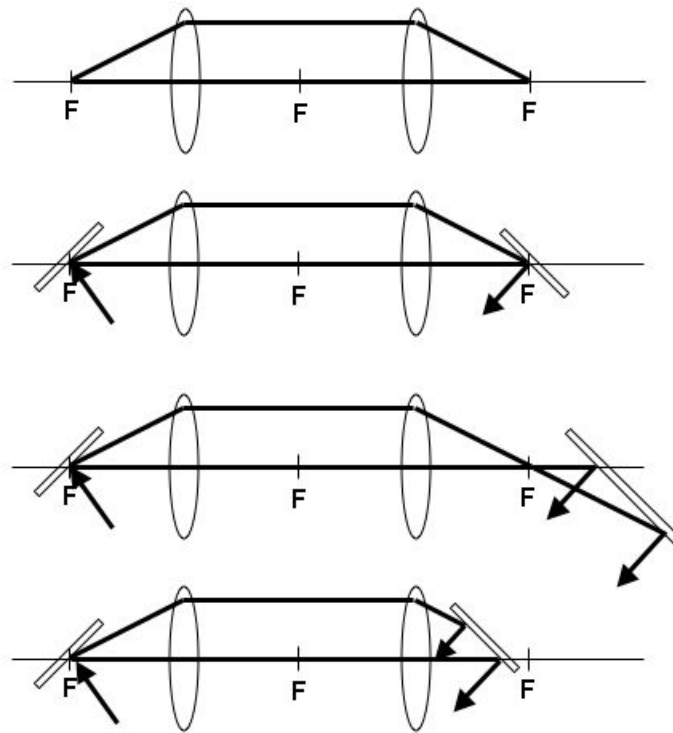


Figure 5 :Using an intra-grating imaging system to control the sign of the dispersion.

A second system capable of delivering large amounts of positive GDD in a compact geometry is an optical fiber, and indeed this formulated the first stretcher in the original CPA system – fiber stretcher, grating pair compressor<sup>5</sup>. This system works, but poses a new challenge. While the magnitude of the GDD provided by the fiber is equal and opposite to the grating pair, the sign of the third order dispersion (TOD) is identical. The TOD from the fiber adds to that generated by the grating pair - thus the system quickly becomes TOD limited, and the pulse compression is poor. (This problem has been solved recently! – more on that later.)

The solution, as discussed earlier, is to use gratings to both stretch and compress. Flipping the sign of the dispersion (to all orders) in a grating pair is accomplished by placing an imaging system within the grating pair compressor. *Figure 5* illustrates exactly how this works. Two lenses of focal length  $f$  are placed  $2f$  apart to form a telescope with negative unity magnification. An object placed at  $f$  in front of the first lens, is imaged at a distance  $f$  behind the second lens (Figure 5a). From Fermat's principle, the pathlength for a ray that travels down the axis of the optical system is identical to that for a ray that is imaged off axis. This basic imaging principle has important consequences for our application. In our case the object and image become gratings. If we place gratings at the object and image points (Figure 5b) and send a short pulse through this system, the net dispersion remains zero – remember, from Fermat all path lengths in this configuration

are identical. In other words the path length traced by the axial ray is identical to that traced by the marginal ray.

Things get interesting, however, if we now push the second grating off the focal point – we can go either direction toward or away from the second lens. If we push the second grating further from the lens, its now at a distance  $f + \Delta f$  and we have the situation shown in Figure 5c. In this geometry there is now a mismatch in path lengths – the axial ray travels a shorter distance relative to the marginal ray. The result: negative dispersion. The net amount of dispersion is identical to that of two gratings separated by a distance  $\Delta f$ .

Similarly, we can push the second grating toward lens two to a distance  $f - \Delta f$  (Figure 5d). Now the axial ray travels a longer path length then the marginal ray – we have created positive dispersion. The net amount of dispersion is identical to that of two gratings separated by a distance  $-\Delta f$ ! Ignoring the effects of aberrations, the dispersion of a grating pair configured in this manner is equal in magnitude and opposite in sign, to all orders, to a normal grating pair.

In principle we now have the ideal stretching and compression system for our CPA laser. A grating pair arranged to provide positive dispersion is used to chirp the pulse to the desired pulsewidth, a second grating pair arranged to provide negative dispersion is used to compress the pulse after amplification.

- **Balancing the dispersion of the stretcher, amplifier material, and the compressor**

All the elements are now in place to create the entire CPA system and we are set to configure the final arrangement of our stretcher and compressor. To do so we need to calculate the net path length for the combination of stretcher and laser amplifier. We will use the result of this analysis to determine the spacing and angle of incidence that is required for our grating compressor. To aid in our understanding, we limit this analysis to include only dispersion through third order. The net group delay through a grating pair in terms of the perpendicular grating separation  $L$ , diffraction order  $m$ , angle of incidence  $\theta_i$ , groove density  $d$ , central wavelength  $\lambda$ , and speed of light  $c$  is

$$GD = \frac{L}{c\sqrt{1 - \left(\frac{m\lambda}{d} - \sin(\theta_i)\right)^2}} + \frac{L \cos\left(\theta_i - \text{Arc sin}\left(\frac{m\lambda}{d} - \sin(\theta_i)\right)\right)}{c\sqrt{1 - \left(\frac{m\lambda}{d} - \sin(\theta_i)\right)^2}} \quad (9)$$

Differentiating this expression, the second order or group delay dispersion (GDD) is

$$GDD = -\frac{\frac{Lm^2\lambda^3}{d^2}}{2c^2\pi\left(\cos(\theta_d)\right)^{\frac{3}{2}}} \quad (10)$$

where  $\theta_d$  is the diffracted angle. Differentiating one more time yields the third order dispersion (TOD)

$$TOD = \frac{3Lm^2\lambda^4 \left( 1 + \cos(2\theta_d) + \frac{2m\lambda}{d} \sin(\theta_d) \right)}{8c^3\pi^2 \left( \cos(\theta_d) \right)^{\frac{5}{2}}} \quad (11)$$

We will walk through a design using typical numbers for a Ti:sapphire system. As before, assuming an input pulsewidth of 30 fs, and a stretched pulsewidth of 100 ps, we can calculate the necessary GDD, and use this number to determine the grating separation for our stretcher. We will use 1200 l/mm gratings in our stretcher and compressor design. These are commonly available gratings that feature good efficiency at 800 nm. Efficiency of these gratings is usually highest at the Littrow angle. Littrow is where the angle of incidence is equal to the angle of diffraction. This is important to keep in mind. We want our compressor to end up as close to Littrow as is practical. We can afford to work off Littrow in the stretcher, efficiency is not as much of an issue there. For the compressor however, we want to avoid throwing as little of our precious amplified light away as is possible.

Littrow angle for 1200 l/mm gratings, at a wavelength of 800 nm is 28.6 degrees. We will choose to use the gratings in our stretcher at 2 degrees off Littrow, 26.6 degrees. Having made a choice of angle of incidence, and having already determined the net amount of GDD required, we place these values into our expression for the GDD and solve for the grating separation. In this case, we calculate a perpendicular grating separation of 28 cm.

The TOD dispersion for the stretcher can now be determined by plugging in our values for grating separation, and angle of incidence. Using the aforementioned values we calculate a value of  $-2.45 \cdot 10^6 \text{ fs}^3$  for our stretcher.

The next step is to take an exact inventory of the amount and type of material our chirped pulse will pass through in our amplifier. In general we have found it very useful in our laser design to limit the number and types of material found in the system. We typically design a system with essentially only three types of material: Ti:sapphire (the amplifier), fused silica (any necessary windows, thin film polarizers, etc), and KD\*P (pockel cells). For a regenerative amplifier based system the net material path length might look something like this: 20 cm Ti:sapphire, 20 cm KD\*P, 5 cm of fused silica. Using the dispersion relations specific for each material, we can now calculate the net path length for the system, and hence the cumulative GDD and TOD due to the amplifier materials. This combination of materials produces  $13146 \text{ fs}^2$  of GDD and  $9607 \text{ fs}^3$  of TOD.

We now add these values to those calculated for the stretcher to find the cumulative GDD and TOD for our system. Note that the sign of the TOD produced by the stretcher is opposite to that produced by the materials – while our cumulative GDD has grown with the addition of the material, the TOD has actually been reduced! For our compressor this means the separation between the gratings will increase (this is our GDD control “knob”) and our angle of incidence will move *closer* to Littrow (this is our TOD control “knob”). Using these cumulative values, setting them equal to our grating GDD and TOD expressions, we solve these equations simultaneously to find our compressor grating separation and angle of incidence. Our cumulative GDD at this point is  $1.169 \cdot 10^6 \text{ fs}^2$  and  $-2.444 \cdot 10^6 \text{ fs}^3$  of TOD. For these values, we end up with a grating separation of

29 cm, and an angle of incidence for the compressor of 27.36 degrees. As predicted, the grating spacing increased, and we moved closer to the Littrow angle where gratings are more efficient.

Now that we have the entire system designed and are ready to construct a CPA laser, it's worth examining how sensitive our system is to various alignment degrees of freedom. We estimate these effects just by examining the GDD term, but in general, if you're really pushing the pulsewidth, the effects of higher order terms should also be considered. This is important to consider, as it will impact the type and design of mounts that we use for the gratings in our system for example. Linear stages with a step size resolution of 10  $\mu\text{m}$  are reasonably available. If we reposition our compressor grating by  $\pm 10 \mu\text{m}$  about the zero dispersion point, our GDD increases by approximately  $\pm 34 \text{ fs}^2$ . This choice of linear stage seems entirely reasonable.

What about angular resolution? If we rotate our grating by  $\pm 1$  degree about the optimal angle, our GDD changes by  $23000 \text{ fs}^2$  (angle change only – separation has been held constant)! This indicates that in general, we want to mount our gratings on stages with an angular resolution substantially better than 1 degree.

The simple analysis described here is normally adequate for designing systems where the stretching/compression ratio is on the order of 1000X and the pulsewidths on the order of 100 fs. If we wish to stretch further, or push the pulsewidth significantly below 100 fs, a more detailed approach is required. For example, up to this point we have neglected the impact of aberrations on our stretcher design. For very large stretching ratios (or equivalently large bandwidths) the imaging optics will be used at or near full aperture. This means that aberrations are no longer negligible, and they can have an impact on the phase of our chirped pulse as well.

### The Offner Triplet – Aberration free stretcher design

It is extremely important in the design of a CPA system to use large aperture optics to avoid spectral clipping that can limit the pulsewidth or change the pulse intensity profile (contrast). As such, the optics are often used at full aperture. As the spectrally dispersed pulse fills the imaging optics spatial aberrations later manifest themselves as temporal distortions when the pulse is compressed. Spherical, coma, astigmatism and chromatic aberrations, can all be problematic.

To eliminate chromatic aberration reflective optics are used in the stretcher. By using an all-reflective triplet design (known as an Offner triplet) all third order aberrations can in fact be eliminated. A stretcher built using this design produces a dispersion that more accurately “mirrors” the dispersion produced by a grating compressor! Its net dispersion is equal in sign and opposite in magnitude.

The aberration free, or Offner triplet stretcher design has been used successfully in ultrashort pulse CPA systems featuring pulses as short as 30 fs<sup>25, 26</sup>. It is capable of large stretching/compression ratios (10,000 X) and has the advantage that these large stretching factors are achieved in compact geometries.

Because the stretcher now matches the compressor dispersion, systems designed using this approach must try to minimize the material path length through the amplifier. Due to the material from the amplifier, the grating compressor distance must be increased (our GDD control knob) and the angle of diffraction increased (our TOD control knob).

This leaves a fourth order mismatch (quartic phase limited) that can limit the compressed pulsewidth. For this reason, an Offner triplet stretcher based system is most suitable for use with multipass amplifier designs as opposed to regenerative amplifier based systems.

### The Cylindrical Mirror Stretcher

The cylindrical mirror stretcher design introduced by Lemoff and Barty<sup>27</sup> is arguably the most successful for ultrashort (<30 fs) CPA systems. As with the Offner design, reflective optics are used to eliminate chromatic aberrations. The choice of cylindrical optics makes it possible to multi-pass the stretcher by conveniently stepping down the beam in height. No tilt is added to the system – in a traditional spherical imaging system this just adds more aberrations but is entirely a nonissue in the cylindrical mirror based design.

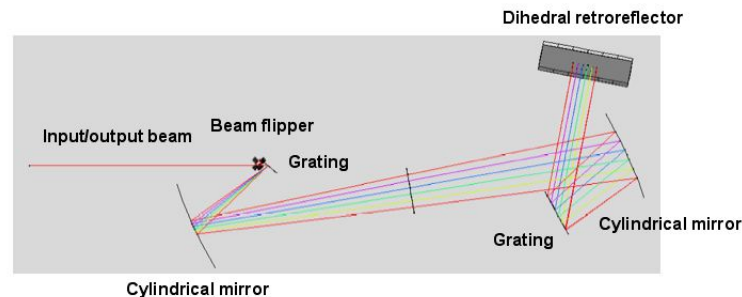


Figure 6 :Ray traced schematic of the Lemoff-Barty cylindrical mirror –based stretcher system.

Tremendous care is taken to minimize spatial inhomogeneities in this stretcher design. For example, a dispersive ray-tracing analysis shows that after one-round trip through the stretcher, the dispersion actually varies as a function of position across the spatial profile of the output beam. In order to eliminate this effect, Lemoff and Barty employed a simple four mirror beam inverter – the beam is flipped about the axis perpendicular to the stretcher plane. The inverted beam is then sent through the stretcher once again. After this second round trip, the dispersion across the beam profile is entirely uniform.

In contrast to the Offner stretcher/compressor design where material path length must be kept to a minimum, the cylindrical mirror based stretcher / compressor system can handle, and indeed requires, large material path lengths. With the correct amount of material this system leaves no residual second, third, or fourth order dispersion – its quintic phase limited.

A second important aspect to this stretcher design is stretched pulsewidth – 20 fs Ti:sapphire CPA systems based on this design have produced stretched pulses > 800 ps.

This has enabled Ti:sapphire amplifiers to be safely operated at fluences of  $2 \text{ J/cm}^2$  and achieve extraction efficiencies right at the theoretical limit<sup>28</sup>.

Notably for these large stretching compression ratios, or large bandwidth systems, no simple analytical solution can be used to find the optimal operating points for the stretcher and the compressor. In these systems dispersive ray-tracing analysis must be employed to design the system and find the exact operating geometry. Critical features in this design include the off-axis angle of the cylindrical mirror telescope that introduces aberrations. The stretcher aberrations are key to the quintic phase limited system operation, as the spatial aberrations alter the spectral dispersion and consequently change the fourth order dispersion of the stretcher.

### Mixed gratings

Wouldn't it be nice to use an aberration-free imaging design and not be limited by material path lengths (fourth order limited)? Aberration-free operation certainly simplifies the initial design procedure – the compressor and stretcher share the identical dispersion relations, the only difference being the sign.

In fact, we have another degree of freedom at our disposal that enables us to take advantage of this design and produce quintic phase limited operation even in the presence of large amounts of material. The “new” parameter –the grating groove density. We are completely free to miss-match the stretcher grating groove density from the compressor grating groove density. By taking advantage of this additional design degree of freedom, Kane and Squier<sup>29</sup> were able to demonstrate that quintic phase limited operation was possible for aberration-free CPA systems even in the presence of large amounts of material such as found in a typical regenerative amplifier based system. For example, by using 1200 l/mm gratings in the stretcher, and 1500 l/mm gratings in the compressor, a 20 fs pulse can be stretched to 450 ps, amplified and compressed to the near-transform limit. This mixed grating approach has proven quite successful, and is featured in many commercially available CPA systems<sup>30</sup>.

### Grisms

The very first CPA system used a fiber as a stretcher and a grating pair as a compressor. Ultimately, as mentioned earlier, this approach was abandoned as the pulse width of the CPA system was reduced, and the miss-match of the fiber dispersion with the grating pair compressor dispersion became the limiting factor. The utility of this original design was never lost however – a fiber is a compact way of stretching a pulse – and methods of modifying the grating compressor to match the dispersion of a fiber were eventually discovered.

The key was to combine two elements, a grating and a prism, to create what is known as a “grism.” Kane and Squier<sup>31</sup> showed that through a judicious choice of grism design, a grism-pair compressor could be designed to compensate for second and third order dispersion from common materials such as fiber. Essentially, the addition of glass into the compressor results in a simple modification of the diffraction equation for a grating

$$n \sin \theta_i + \sin \theta_d = \frac{m\lambda}{d} \quad (12)$$

The appearance of the index of refraction of the glass media in the equation enables the grating to diffract at angles that were previously prohibitive. At these new angles, the sign of the third order dispersion of the grism compressor is actually reversed – it becomes negative. Thus through proper design a grism compressor can simultaneously compensate for second and third order material dispersion. A fiber stretcher, amplifier, grism compressor was demonstrated<sup>32</sup> and used to produce 135 fs pulses. The limitation of this design was the efficiency of the grisms. Today this is a non-issue as grisms exhibiting diffraction efficiencies >90% are commercially available.

Current systems use grisms in a slightly different modality. In order to simplify the laser system and minimize the alignment degrees of freedom, grisms are used as the stretcher, and a large piece of antireflection coated glass is used as the compressor. Because negative dispersion is now used to stretch, and positive dispersion is used to compress, this system is known as a Down Chirped Pulse Amplification (DCPA) system. In addition to the compact architecture and dramatically reduced alignment complexity of this system, one of its strengths is the efficiency of the AR-coated glass compressor – it can be 98% efficient. By comparison, a typical grating compressor is 60-70% efficient. Gibson et al<sup>33</sup>, and Gaudiosi et al<sup>34</sup> have used this design to produce 200 μJ, 35 fs pulses at a repetition rate of 5 kHz. For pulse energies in the microjoule range, the grism stretcher / glass compressor is an outstanding design alternative.

### III. Amplification

Now that we are familiar with the basics of stretching and compressing, we can do a few simple calculations to help aid designing of the actual amplifier. Let's consider a typical case of an amplifier that brings a stretched input pulse energy from  $E_{in} = 1$  nJ to an output energy of  $E_{out} = 1$  mJ. We'll see how the optical arrangement of the amplifier is constrained by the parameters of the system. First, as mentioned earlier, it is important to saturate the amplifier for good efficiency. (Dependent on the amplifier design, this will also impact the shot-to-shot pulse stability.) This will happen if the output fluence is close to or higher than the saturation fluence,  $F_{sat} = \hbar\omega / \sigma_{21}$ . Since  $F_{sat}$  is determined by the gain medium, you can see that the beam size in the amplifier is determined by the desired output energy. In Ti:sapphire,  $F_{sat} \approx 0.84$  J/cm<sup>2</sup> @ 794 nm<sup>35, 36</sup>, so for  $E_{out} = 1$  mJ, the  $1/e^2$  beam radius would be roughly  $r = 180$  μm. (Since the Rayleigh range at  $\lambda_0 = 800$  nm for this beam is only 12.5 cm, some sort of focusing optics will be necessary to maintain the beam size from pass to pass.) How many passes will we need? The small-signal, single pass gain is determined by the pump fluence  $F_{pump}$ :  $G_0 = \exp[F_{pump} / F_{sat}]$ . We can estimate the number of passes by seeing how many passes ( $N$ ) are required to bring the pulse fluence up to the saturation fluence:  $E_{out} \approx E_{in} G_0^N \approx F_{sat} A$ , where  $A$  is the beam area. For  $G_0 = 5$ , the input pulse should reach saturation after 8-9 passes through the crystal, assuming there are no losses. You can see that if the gain is low, we will need to make the beam take many passes through the crystal. At  $G_0 = 2$ , the number of passes required is around 20. In general in cases where the saturation fluence is high or the per

pass gain is low, a regenerative amplifier geometry is desirable. For high gain, low saturation fluence systems, a multipass geometry can be advantageous.

A second stage, power amplifier often operates under slightly different constraints – no imaging optics are required for each pass through the crystal. For example, starting with 1 mJ from the first stage, and amplifying to 100mJ, the final beam size is on the order of 3.5 mm diameter. The rayleigh range of this beam is sufficiently long that the beam can multipass the power amplifier (say 4 passes) by simple bow-tie configurations that only require flat turning mirrors.

- **Regenerative Amplifiers for CPA**

In Figure 3, it was shown that it is desirable to operate at approximately twice the saturation fluence to optimize extraction efficiency. However, for many materials the saturation fluence is simply too high to be reached given the restriction that is in general impractical to stretch the pulse beyond 1 ns. In other words, because of the limitation in our stretched pulse duration, we'll reach the damage threshold of the system before we can hit the saturation fluence.

A regenerative amplifier is a clever method of getting around this limitation. Basically, we can still achieve high extraction efficiencies even if we operate at fluences well below the saturation fluence – we just have to multipass the gain media. The great utility of the regenerative amplifier is it enables an arbitrary number of passes through said media. However many passes are required to fully extract the energy stored in the amplifier, be it 10 or 100, the regenerative amplifier is happy to accommodate. Not surprisingly, the highest extraction efficiency CPA systems are in general regenerative amplifier based.

The basic regenerative amplifier configuration is illustrated in *Figure 7*. The cavity is nominally a stable resonator design, though unstable resonators have also been used. In this chapter we will focus only on the stable resonator. There are only three primary components in the resonator: a Pockels cell, thin-film polarizer and the gain media. The combination of the Pockels cell and thin-film polarizer are used to shuttle the pulse into and out of the resonator. The gain media and thin film polarizer are aligned centered on the axis of the cavity, the Pockels cell is slightly tilted with respect to the cavity axis to provide a static quarter wave of birefringence. This has important consequences for the amplifier operation. With the Pockels cell off, any light emitted by the gain media is coupled out of the resonator, and any external pulses that enter the cavity are rejected after one round trip.

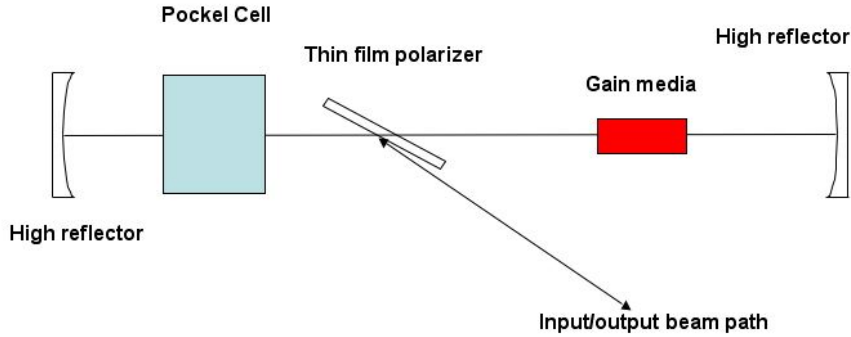


Figure 7 : Basic regenerative amplifier configuration.

Operation of the amplifier proceeds along the following sequence. The pump laser fires, and the pump laser light is absorbed by the gain media. The Pockel cell is timed such that it remains off until the energy from the pump laser is fully absorbed and the fluorescence emission from the gain media is peaked. At this peak and after the chirped pulse has entered the cavity, a quarter-wave voltage is applied across the Pockel cell for a net half wave of retardation. The chirped pulse is now “trapped”. The pulse passes through the gain media two times per round trip, extracting energy with each pass. The quarter-wave voltage is maintained across the Pockel cell for as long as is required for the pulse to fully extract the stored energy. For a Ti:sapphire regenerative amplifier, this is typically 10-15 round-trips (20-30 passes through the Ti:sapphire). Once the maximum amount of energy is in the chirped pulse, the voltage across the Pockel cell is increased by another quarter-wave, for a net retardation of three quarter wave. (The Pockel cell voltage is typically increased by an additional quarter-wave rather than discharged to zero as the rise time is much faster (on the order nanoseconds) than the decay time (microseconds).) Upon double passing the Pockel cell the chirped pulse experiences a net half wave retardation, its polarization is changed from p to s, and the pulse is rejected from the resonator.

The pulse build up inside a regenerative amplifier can be modeled quite accurately by following the development of Lowdermilk & Murray<sup>24, 37</sup>

$$F_{out}^{(k)} = F_{sat} \ln \left\{ 1 + G_0^{(k)} \left[ \exp\left(\frac{F_{in}^{(k)}}{F_{sat}}\right) - 1 \right] \right\} \quad (13)$$

$F_{out}^{(k)}$  is the output pulse fluence for the  $k^{\text{th}}$  pass in terms of the saturation fluence,  $F_{sat}$ , the small signal gain,  $G_0^{(k)}$ , and the input fluence,  $F_{in}^{(k)}$ . The small signal gain is given in turn by the expression

$$G_0^{(k)} = \exp\left[\frac{F_{stored}^{(k)}}{F_{sat}}\right] \quad (14)$$

where  $F_{stored}^{(k)}$  is the stored energy. These equations are applied iteratively, the stored energy decreasing as the energy is extracted with each pass through the amplifier

$$F_{stored}^{(k+1)} = F_{stored}^{(k)} - F_{out}^{(k)} + F_{in}^{(k)} \quad (15)$$

The input for the next round trip (k+1) is related to the output from the previous roundtrip (k) by the net transmission T of the amplifier

$$F_{in}^{(k+1)} = TF_{out}^{(k)} \quad (16)$$

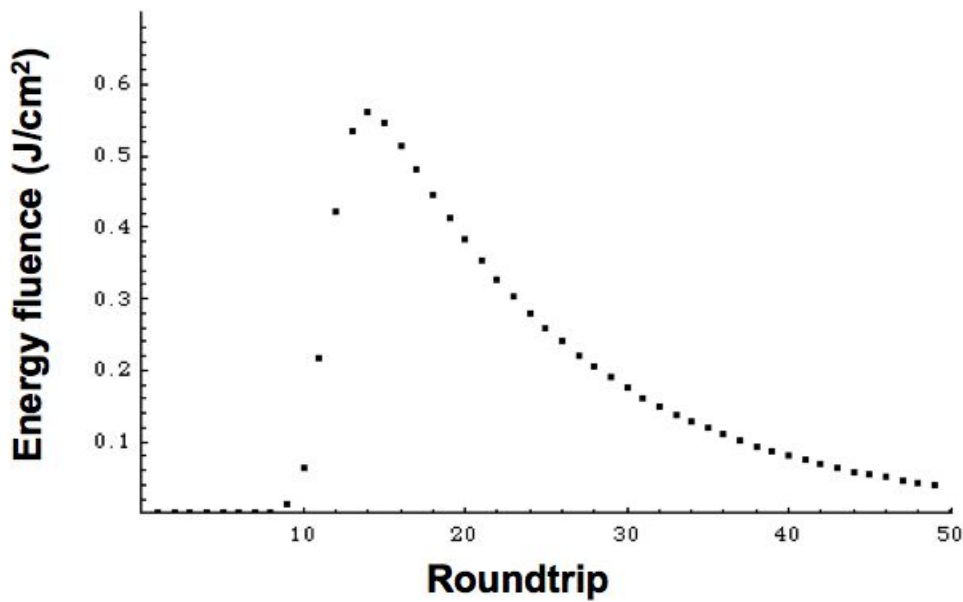


Figure 8 : Energy buildup (expressed as fluence) as a function of roundtrip for the parameters listed in the text.

*Figure 8* models the buildup using the above analysis for a typical kilohertz repetition rate Ti:sapphire regenerative amplifier. The injected energy of the chirped pulse is assumed to be 10 pJ. In a real regenerative amplifier, the pulse is kicked out of the cavity at the peak energy or within one roundtrip after the peak. The plot in *Figure 8* tracks the pulse after the peak- the pulse begins decaying back to zero after 17 roundtrips. After 17 roundtrips the roundtrip gain no longer exceeds the roundtrip losses, and as can be seen from the plot if the pulse remains in the resonator it begins to decay to zero.

These numbers compare quite favorably for the system reported by Rudd et al.<sup>38</sup>, where we assume round trip losses of 7.5%, and the pump spot size/ volume perfectly matches the resonator mode within the rod. The model predicts a maximum pulse energy of 1.5 mJ, which is in good agreement with the measured value of 1.2 mJ given these assumptions.

The model can be further refined to include spatial variations in the gain, and is particularly important to do so when modeling power amplifiers<sup>39</sup>. A model that includes spatial effects will also describe the gain shaping of spatial profiles (detailed in following section). As with all amplifiers, gain narrowing and gain saturation is an important issue with regenerative amplifiers and leads to a reduction in the amplified bandwidth. These issues are covered in the section on multipass amplifiers, as well as methods for overcoming the gain narrowing.

- **Multipass Amplifiers**

An alternative to the regenerative amplifier is the multipass amplifier. As you would guess from the name, a multipass amplifier has no resonator: the seed pulse is passed through the gain medium several times until the energy is extracted. The optical configuration is largely determined by the net gain required and the number of passes that will saturate the gain. One or two passes through the gain is easy; 8 or 12 passes requires a clever optical design. Both situations arise in typical systems. In the first stage of amplification, a pulse is amplified from the nJ to mJ level. The net gain ( $10^6$ ) is high, but since the output pulse energy is small, the efficiency is not critical. Many of these preamplifiers are followed by one or more power amplifiers. A power amplifier might take the pulse energy from 1 to 10 mJ: the net gain is low, but we must have high extraction efficiency to make economical use of the pump power.

The architecture of a power amplifier, with up to 4 passes, depends on the properties of the gain medium. Let's illustrate this by considering two gain media: Nd:YAG and Ti:sapphire. Nd:YAG is typically flashlamp-pumped from the sides of a long (3-4cm), narrow (~10mm) rod. The aspect ratio of the rod is such that the beam must propagate straight through the rod to avoid clipping the rod edges, but since the YAG crystal is not birefringent, a quarter wave plate may be double-passed to allow the beam to take two passes without an angle between them. With the addition of a Faraday isolator and another mirror, 4 passes can be taken without any active switching. For our other example, sapphire is birefringent, with much stronger gain along one axis, so polarization switching won't work. However, Ti:sapphire is laser-pumped from the end, and the crystals are much shorter in length, so we can use several mirrors to force the beam to take the required number of passes through the crystal. This "bowtie" configuration is common for Ti:sapphire power amplifiers, but the high mirror count increases the sensitivity to misalignment, so it would be impractical for many more passes.

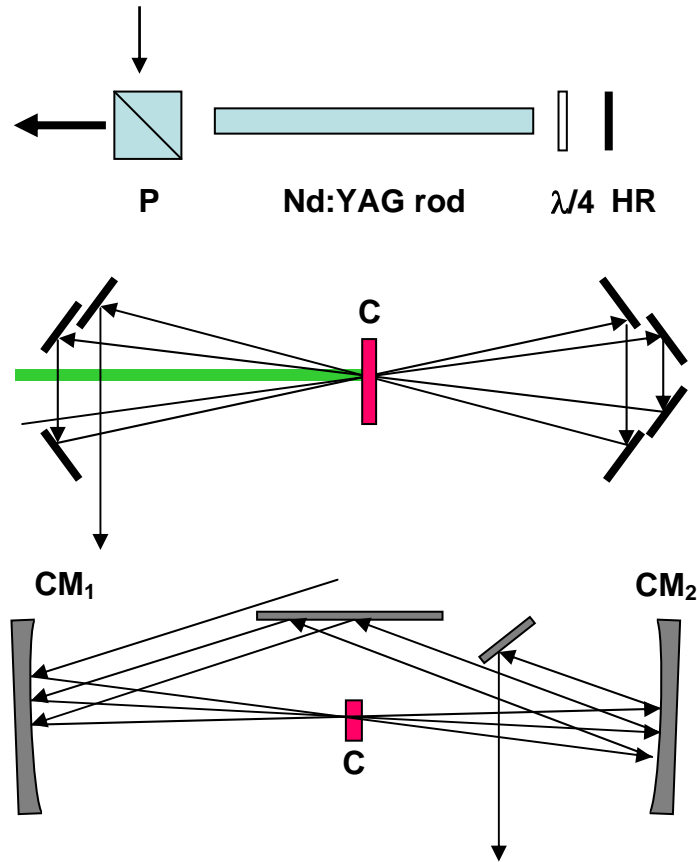


Figure 9 : a) Double-pass amplifier in a non-birefringent, low-gain/cm medium such as Nd:YAG. B) Four-pass bowtie amplifier. C) 3-mirror ring amplifier; only 3 passes are shown for clarity.

Several optical configurations have been demonstrated that allow multiple passes through the crystal. One of these, a 3-mirror ring, is shown in *Figure 9*. Two curved mirrors ( $CM_1$ ,  $CM_2$ ) are placed confocally with the crystal at the focus. If these mirrors are aligned to face each other, the beam can take at most two passes before the beam retraces its path. We introduce a tilt on each mirror ( $\theta$ ) along with a long flat mirror  $M_1$  as shown in the figure. If the distance between the crystal and the flat mirror is  $f \tan 2\theta$ , a beam that passes through the crystal will complete a ring. However, if we push  $M$  closer to the crystal by a distance  $\Delta y$ , the second pass will strike  $M$  at a point farther to the right, reflecting the beam parallel to the input. Each subsequent trip passes through the crystal incremented by an angle  $\Delta\alpha = 2\Delta l/f$ . Note that if the input beam is collimated it will be brought to a focus in the crystal by  $CM_1$ . With  $f = 500\text{mm}$ , and the  $R = 180\mu\text{m}$  beam radius in the crystal as described above, the beam size on the mirrors will have a  $1/e^2$  diameter of approximately 1.5mm. This beam is recollimated by  $CM_2$  and reflects off  $CM_1$  for another round trip. With mirror  $M$  4" long, it is possible to get 8 passes through the crystal while still having sufficient beam separation to get the beams in and out cleanly.

Since there is no need for pulse switching inside a multipass amplifier, it is possible to design the amplifier with very little path through optical material. With aberration-free

stretching and compression, recompression is significantly more difficult when the net material dispersion is high. The linear cavity of the regenerative amplifier also allows for stray reflections from the polarizer to propagate in the output direction, which leads to prepulses that may be detrimental to the application or experiment. Prepulses in a multipass amplifier are limited to the leakage from the intracavity polarizer. Along with this slight advantage in pulse characteristics is an increase in the care required to maintain a good output beam quality. A well-designed regenerative amplifier operates with a near-Gaussian output mode that is insensitive to the mode of the seed beam. In a multipass amplifier, the output beam quality is determined by the input beam profile, the optics in the amplifier, the gain profile, and thermal lensing. The input profile can be improved, if necessary, by spatial filtering. Many multipass designs contain curved mirrors that are not used at normal incidence. When a mirror is tilted, the horizontal and vertical planes have different focal lengths:  $f_H = f_0 \cos \theta$ ,  $f_V = f_0 / \cos \theta$ . A certain amount of astigmatism can be compensated with optics downstream, for example with the output telescope that enlarges the beam before the compressor. One of the design considerations for the multipass is to minimize the astigmatism, typically by keeping the mirror separations sufficiently large so that the mirror tilt angles can be small. Gain shaping of the spatial profile and thermal effects will be treated in the following sections.

- **Gain shaping of spatial and spectral profiles**

In the simplest model of the amplification process, the laser crystal has a uniform gain spatially across the input beam, and the entire spectrum of the input will experience the same gain. Of course, life isn't so simple, and the variability of the spatial and spectral gain profiles has real consequences for the amplifier performance. In both cases, peaking of the gain toward the center of the profile tends to narrow the width of the profile.

As we look at spatial shaping of the amplified beam that results from the gain distribution, let's first understand how the single-pass gain profile is affected by the pump and seed fluences. While the gain shaping effects are important in all pumping configurations, we'll use the computationally simple example of a longitudinally laser-pumped crystal, where stored fluence follows the pump beam profile. The small signal single pass gain is  $G(r) = \exp[F_{stor}(r)/F_{sat}]$ , which for a Gaussian pump profile is

$G(r) = \exp\left[F_{stor} e^{-2r^2/w_p^2} / F_{sat}\right]$ . For small gain ( $F_{stor} / F_{sat} \ll 1$ ), we can make an approximation on the first exponential to show that the amplification follows the pump profile:  $G(r) - 1 = F_{stor} e^{-2r^2/w_p^2} / F_{sat}$ . At high gain, the gain profile is narrower and is no longer Gaussian. At high seed fluence, we can use the Franz-Nodvik equations to account for gain saturation. At an input fluence equal to the saturation fluence, the gain profile is very close to that of the pump. Of course, pump beams, especially those from flashlamp-pumped systems, are not symmetric. The actual pumping distribution in the crystal can be measured by projecting an image of the fluorescence to a camera along the direction of the seed beam. For a wide bandwidth gain medium, this can be accomplished by using an interference filter centered at a wavelength far from the gain peak.

The effect of spatial gain shaping is typically not large on a single pass, but in a multipass amplifier, the effects can accumulate. In the general case, a model of the process would first account for spatial narrowing of the beam in the crystal, then use Fresnel diffraction integrals to propagate the output beam from the crystal through the system to return to the crystal with a new beam profile. In several of the amplifier configurations, however, each pass through the crystal is relay-imaged, so the input to each pass is the same profile as the output of the previous pass. The net effect is illustrated in Figure 10: the beam size decreases during amplification, leading to saturation in the center of the gain profile and a reduction in the extraction efficiency. If the gain narrowing effect is not strong, saturation will pull the beam profile back, otherwise the system can be designed to provide magnification or the pump profile can be shaped to give a flatter distribution.

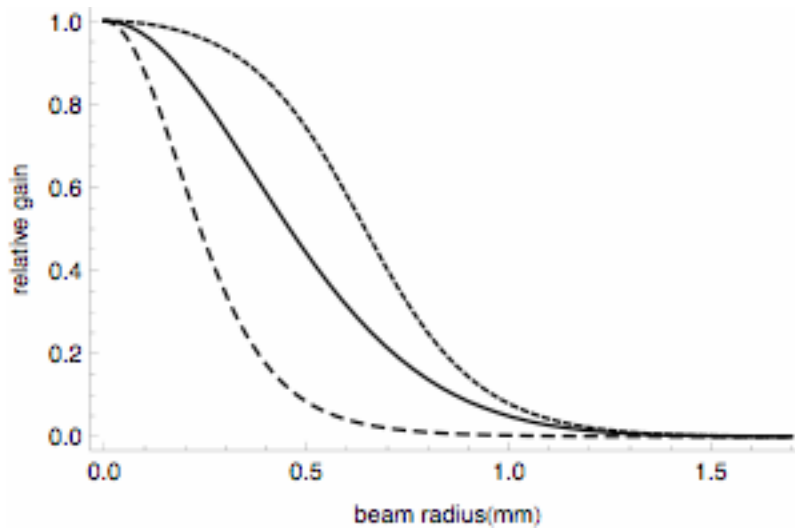


Figure 10: Calculated beam profiles for different passes in a multipass, relay-imaged amplifier. Small dash: seed beam is the same size as the Gaussian-profile pump. Early passes (solid, large dash) show spatial gain narrowing, while the saturated, last pass shows the effect of saturation.

Gain narrowing and shaping effects are also seen in the spectral domain. Here it is the spectral dependence of the stimulated emission cross-section that leads to a variation in the saturation fluence with wavelength:  $F_{sat}(\omega) = \hbar\omega / \sigma(\omega)$ . The resulting narrowing of the spectrum during amplification limits the output pulse duration substantially. At present, titanium-doped sapphire is the gain medium with the widest spectral bandwidth, extending from 650nm to 1100nm<sup>36, 40</sup>. Such a wide bandwidth can support the generation of pulses less than 5fs in duration. While, laser oscillators have recently been developed that reach that limit, gain narrowing is the current limitation in preserving this wide bandwidth during amplification to the mJ energy level and beyond.

In the small-signal gain limit, ignoring for now losses and saturation effects discussed below, the amplified (output) spectrum is given by:

$$I_{out}(\omega) = I_{in}(\omega)[G_{RT}(\omega)]^N, \quad (17)$$

where  $G_{RT}(\omega)$  is the round-trip gain and  $N$  is the number of amplifier round trips. In the spatial case, we found above that saturation could compensate the reduction in the beam size. However, in homogeneously broadened gain media, the linewidth of each atom

participating in the amplification process is broadened, and gain saturation cannot bring up the amplitude of the spectral wings. Without losses in the amplifier, the amplified spectral width FWHM (full-width at half maximum) is approximately  $\Delta\omega = \gamma / (\ln G_{tot})^{1/2}$ , where  $\gamma$  is the FWHM of the gain curve of the medium (120nm for Ti:Sapphire<sup>41</sup>, and  $G_{tot}$  is the total energy gain of the amplifier. At the several mJ energy level, gain narrowing restricts the pulse duration to a minimum in the 30-35fs range. At higher energies, this minimum increases further. Moreover, there are many other broadband gain media (for example Yb:KGW, Cr:LiSAF, Cr:Forsterite) that operate in useful parts of the spectrum and can be pumped efficiently by laser diodes. While unable to compete with Ti:sapphire for the shortest pulses, a means to counteract gain narrowing would extend the range of pulse durations that can be achieved with these systems.

For a given value of  $G_{tot}$  (corresponding to the desired output energy), losses tend to increase the gain narrowing effect. If  $L_{RT}$  represents the loss on each round trip, the amplified spectral width is reduced:  $\Delta\omega = \gamma / (\ln G_{tot} - N \ln(1 - L_{RT}))^{1/2}$ . Systems with higher gain/pass and lower losses (e.g. multipass amplifiers) will generally amplify wider bandwidth without correction. We should also point out that narrowing of the spectrum also occurs as a result of the limited bandwidth of the dielectric mirrors in the system. If damage thresholds permit, silver mirrors may be used. The bandwidth of dielectric mirrors reflecting at 45° is substantially greater for *S* polarization instead of *P*. In a multistage system, the majority of the gain narrowing will clearly occur in the first, high-gain stage; this is where correction should be applied.

Gain saturation in a CPA system has the effect of pulling the spectrum toward the part of the spectrum that is on the leading edge of the chirped pulse. When the input fluence is near or greater than the saturation fluence, the leading edge of the pulse experiences more gain and robs the stored energy from the back of the pulse. This effect can pull the spectrum by 10-20 nm. The shifting is not inherently a problem, though it may push the spectrum toward the edge of the reflectivity range of the mirrors. Examples of gain narrowing and frequency pulling are shown in *Figure .*

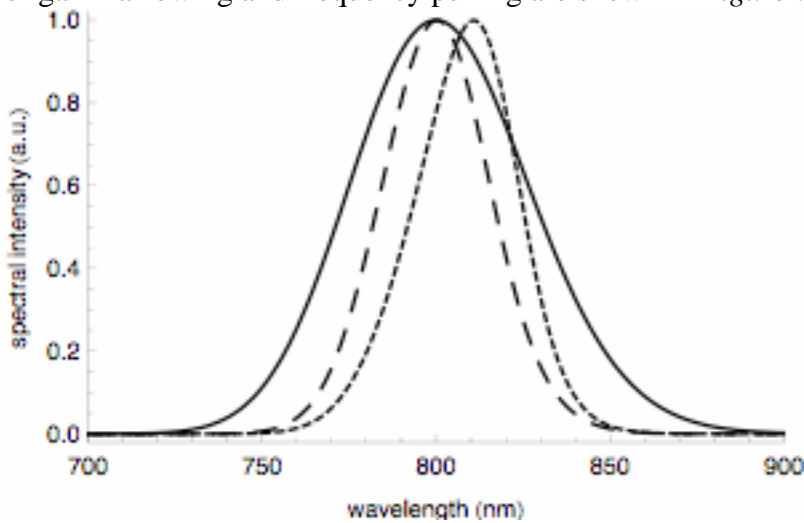


Figure 11 : Calculated spectral profiles during amplification. Seed pulse spectrum for a 10fs pulse is narrowed by amplification in a low-gain, first stage amplifier. Strong saturation in a second-stage amplifier leads to pulling of the spectrum toward long wavelengths.

Reaching the shortest amplified pulses is one motivation for being able to shape the amplified spectrum. Since gain narrowing reduces the duration of the stretched pulse, it increases the risk of mirror damage and the accumulation of nonlinear phase ( $B$ -integral). Pulse shaping and synthesis would also be greatly enhanced with the availability of greater bandwidth. With control over the spectral shape of the net system gain, amplification at wavelengths away from the gain peak is possible while avoiding pulling of the spectrum toward the gain peak. An example of this would be amplification of  $>850\text{nm}$  pulses in Ti:sapphire. Simultaneous amplification of different pulses at different wavelength peaks is another application. Since the pulses could be derived from a single wide bandwidth seed, the automatic synchronization enables difference frequency mixing for far IR pulse generation<sup>42</sup>.

In principle, it is possible to pre-shape the spectrum of the input pulse  $I_{in}(\omega)$  to yield a wider-bandwidth output pulse. Modification of the round-trip gain of the amplifier is preferred: pre-shaping the seed spectrum leads to a low-energy seed and leaves the gain for the amplified spontaneous emission (ASE) unaffected. A lossy element placed inside the amplifier, regeneratively shaping the spectrum, will filter the seed and ASE equally. The simplest method is to use a thin, uncoated pellicle as an etalon, positioning a dip in the spectral transmission to be at the peak gain wavelength. The width of the transmission dip is determined by the thickness of the pellicle. More recently, a dielectric coated filter with high damage threshold has been demonstrated. With these techniques, bandwidths for amplified pulses compressed to  $<20\text{fs}$  have been demonstrated<sup>43, 44</sup>.

- **High average power ultrafast systems**

Since many applications and experiments require modest pulse energy but can improve with increased repetition rates, high average power ultrafast systems are becoming more common. Since these systems are pumped with lasers that are continuously-pumped and Q-switched, the pulse-to-pulse fluctuations are very low. Arc-lamp pumped pump lasers are gradually being replaced with diode-pumped lasers.

For the ultrafast amplifier, the primary design issue to address is the thermal load in the crystal. The end result is that the thermal gradients induced in the crystal by the pump lead to the creation of a lens for the amplified beam. These effects are well-described in Koechner<sup>45</sup>. Management of this issue is best described in terms of several individual factors. Each of these factors will contribute a different amount for the different gain media and amplifier configurations.

- 1) *Generation of the heat load:* The photon energy of the pump is necessarily larger than that of the amplified beam, and the residual energy is left in the crystal as heat. The ratio  $\Gamma = \omega_{seed} / \omega_{pump}$ , which represents the theoretical maximum efficiency in the amplifier, is about 0.66 for Ti:sapphire pumped at 532nm, but can be quite low in some systems such as Ytterbium-doped lasers ( $\sim 0.95$ ).
- 2) *Thermal gradients in the crystal:* Given the heat load and the cooling geometry, the finite thermal conductivity of the medium leads to a temperature gradient in the crystal. For the most common, transverse cooling geometry, where the crystal is

cylindrical in shape and is cooled on the barrel, the temperature decreases outwards from the center of the pumped region. In the general case, this temperature distribution can be calculated from the heat equation, but in the simple case of uniform heat distribution, the temperature evolves into a parabolic distribution:

$T(r) = T(r_0) + \frac{Q}{4K}(r_0^2 - r^2)$ , where  $Q$  is the rate of heat generation/volume,  $K$  is the thermal conductivity, and  $r_0$  is the radius of the rod. Values of the thermal conductivity among the gain media used in ultrafast systems vary widely, from  $\sim 1.0$  W/m/K for glass to  $\sim 35$  W/m/K for sapphire. Note that the actual temperature of the coolant does not appear to affect the gradient, but in general the thermal conductivity is a function of the temperature. The success of cryogenic systems described below relies in part on the decrease of  $K$  with temperature.

- 3) *Cooling time*: In the typical geometry, the heat is removed from the laser rod from its circular boundary. At very high repetition rates for pumping, the timescale for cooling is sufficiently slow that the thermal distribution reaches the continuous wave limit of the profile described above. However, under some circumstances, the crystal will cool during the time between pump pulses, and the thermal gradients are diminished compared to the CW limit. There are several timescales in the process: the optical pump pulse duration  $\tau_{\text{pump}}$ , the transfer of some of the pump energy to heat in the crystal  $\tau_{\text{heat}}$ , the amplifier extraction time  $\tau_{\text{ext}}$ , the timescale for thermal conduction of the heat out to the rod walls,  $\tau_{\text{th}}$ , and the interval between pump pulses,  $1/\nu_{\text{rep}}$ . The typical ordering of these time scales is  $\tau_{\text{pump}} < \tau_{\text{heat}} \approx \tau_{\text{ext}} < \tau_{\text{th}}, 1/\nu_{\text{rep}}$ .

When  $\tau_{\text{th}} \gg 1/\nu_{\text{rep}}$ , we can treat the input pump beam as depositing a continuous average power. The timescale  $\tau_{\text{th}}$  is determined by the solution of the heat equation,  $\partial T/\partial t = \kappa \nabla^2 T$ , where  $\kappa = K/C$  is the thermal diffusivity, and  $C$  is the specific heat. Assuming a cylindrical symmetry and a uniform pump beam, the solution is a sum of Bessel functions, and the slowest cooling timescale is  $\tau_{\text{th}} \approx r^2/\kappa c_{01}^2$ , where  $c_{01}$  is the first zero of the  $J_0$  Bessel function.

- 4) *Effects of  $dn/dT$* : The thermal dependence of the refractive index is the primary contributing factor to thermal lensing. The thermal gradient turns the crystal into a gradient-index lens:  $f \approx \frac{2K}{I_{\text{avg}} n_0 dn/dT}$ , where  $I_{\text{avg}}$  is the portion of the absorbed

pumping intensity given off as heat in the crystal per second. For most laser materials,  $dn/dT$  is positive, resulting in a focusing effect, which can be quite strong at high repetition rates. Below we will work out an example for the thermal lens, but let's see what determines the value of the  $I_{\text{avg}}$ . Suppose we have a given pump fluence per shot,  $F_{\text{pump}}$ . The stored fluence is  $F_{\text{stor}} = \Gamma F_{\text{pump}}$ , and the single pass gain is  $G_0 = \exp(\Gamma F_{\text{pump}} / F_{\text{sat}})$ . With the theoretical maximum extraction efficiency, the energy fluence left in the crystal for each shot would be  $(1 - \Gamma)F_{\text{pump}}$ . But not all the

stored energy will be extracted, so we add to this fluence  $\eta \Gamma F_{pump}$ , where  $\eta$  is the efficiency of extraction of the stored energy. Finally, we can write  $F_{pump}$  in terms of the desired single pass gain and use the repetition rate  $R$  to get

$I_{avg} = R \ln(G_0) F_{sat} [(1/\Gamma) - (1 - \eta)]$ . Writing the expression in this way makes clear the role of the saturation fluence and the quantum defect for the laser material. Also note that the thermal effects will have larger role in higher-gain multipass systems compared to regenerative amplifier systems that are typically operated with lower single pass gain.

- 5) *Thermal expansion effects:* Thermal gradients lead to expansion gradients that stress the crystal. At the extreme limit, the rod can fracture. The stress fracture limit for the dissipated power per unit length of rod ranges from 25 W/cm for glass to 2.5 kW/cm for sapphire. While the doping level can be adjusted down for weaker materials such as glass to distribute the thermal load over a longer rod length, only the harder host crystals such as sapphire or YAG are suitable for high average power systems. Even below the fracture limit, the thermal expansion leads to lensing from the bowing of the rod surfaces and stress-induced refractive index changes. The contribution to the

thermal lens from this effect is  $f \approx \frac{2K}{I_{avg} (n_0 - 1)\alpha}$ , where  $\alpha$  is the thermal expansion

coefficient. This contribution to thermal lensing is typically not as strong as that from the thermal dependence of the index of refraction described below. The radial variation of the thermal gradient also results in different values for the induced stress in the radial and azimuthal directions. The variation of refractive index with stress sets up a birefringence that is typically not important in materials that are already birefringent, but is significant in isotropic media such as glass and YAG.

#### *Elimination of the thermal lens: cryogenic cooling*

In the presence of a large heat load, we can either compensate for the thermal lens, or we can try to eliminate the lens by using cryogenic cooling or a different cooling geometry. In a regenerative amplifier, the cavity is designed around a stable mode. Treating the rod as a lens, the cavity can be designed to not only give a stable mode, but to reduce the sensitivity of the cavity to changes in the thermal lens. This approach can be applied to a multipass amplifier<sup>46</sup>. Even though the multipass is not a resonator, it can be considered as a ring cavity with an internal lens.

While the performance of the thermal eigenmode amplifier was excellent, many have chosen the path of eliminating the thermal lens through cryogenic cooling. As shown above, the properties of sapphire are greatly improved with cryogenic cooling. Either liquid nitrogen or a closed-cycle chiller is used for cooling, and great care must be taken in the cryostat design to ensure that the cooling is symmetric around the beam path. The vacuum must be oil-free and sufficiently low ( $\sim 10^{-8}$ - $10^{-7}$  Torr) to avoid condensation on the crystal faces.

The temperature dependent parameters that are affected by cooling are the thermal conductivity, the rate of change in refractive index with temperature,  $dn/dT$ , and the specific heat. The strength of the thermal lens is proportional to  $K/(dn/dT)$ , while the cooling rate is proportional to  $K/C_p$ . These parameters are plotted in Figure 12, showing the dramatic beneficial effects of cryogenic cooling in sapphire. Even at 1 kHz, there can be substantial cooling of the profile between shots when the crystal is at low temperature. The amplified pulse experiences the temperature profile that is present at the end of the last pulse; cooling reduces the thermal gradients and the amount of lensing at the same time.

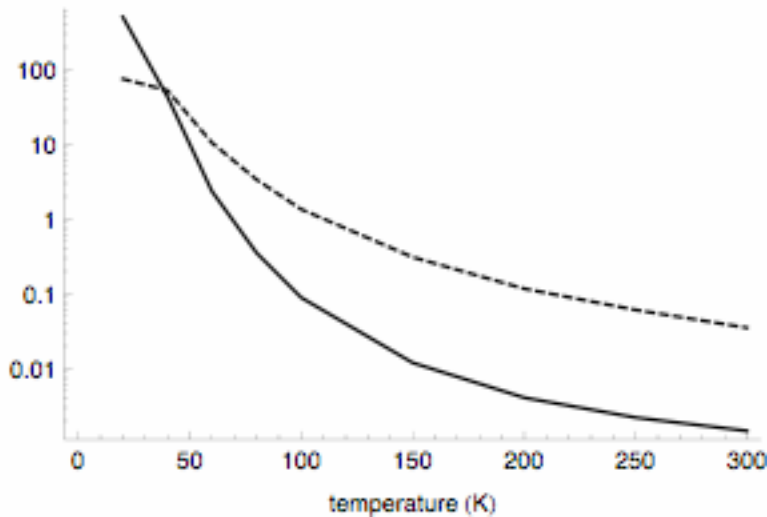


Figure 11 :Temperature dependence of thermal properties of sapphire. Dashed: ratio of  $K/(dn/dT)$ , which determines the thermal lens focal length. Solid: ratio of  $K/C_p$ , which is proportional to the cooling rate.

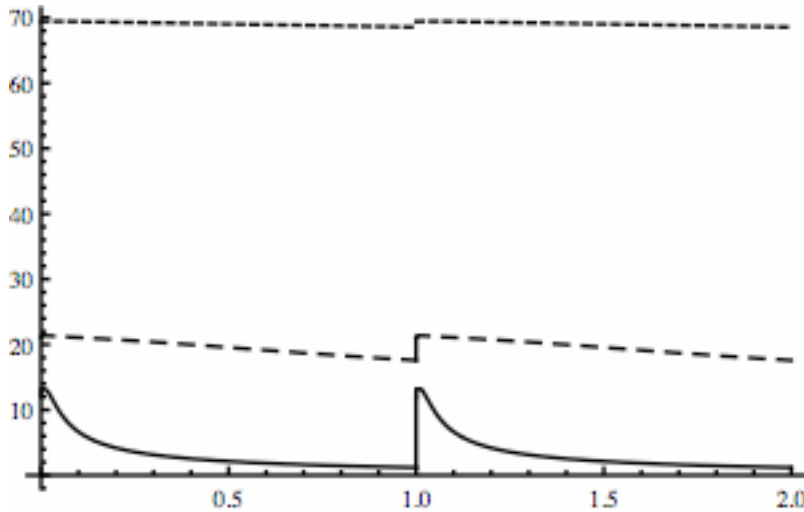


Figure 12 : Value of  $T(0, t) - T(a)$  for repetitive pumping at 1 kHz after settling of initial transients.  $T(a) = 300K$  (small dash),  $120K$  (large dash),  $77K$  (solid line).

Before leaving this subject, we should mention that another alternative is to use thin-disk cooling, a technique that has been successfully used with diode-pumped Yb:YAG oscillators<sup>2</sup>. In this case, the crystal is coated with a mirror coating on the back end, and

is optically pumped from the front. The heat sink is on the back, so the thermal gradients are predominately along the direction of the beam, eliminating thermal lensing.

#### **IV. Adaptive optics: focusing CPA pulses**

The preceding sections described the amplification process in a CPA system and emphasized the importance of controlling dispersion and spectral bandwidth of the laser pulse during the amplification. At the end of a CPA system, the compressor brings back the pulse to its minimal duration by minimizing the residual spectral phase. This ensures optimal “focusing” of the pulse in the time domain. In order to achieve the highest intensities, the femtosecond laser beam is often focused to a small spot using all-reflective optics, such as an off-axis parabola. Using a refractive optic as focusing element is, in general, not practical as the dispersion of the material would broaden the temporal profile and possibly induce unwanted nonlinear effects due to the B-integral.

The spatial distribution of the focal spot will be influenced by the presence of spatial phase aberrations, just as the temporal profile was affected by uncompensated spectral phase terms (GDD, TOD, ...). This section will deal with correction of these spatial phase (or wavefront) aberrations using active, or adaptive optics. In a CPA system, propagation through the many numerous optical components, non-linear effects occurring in the amplifying medium, inhomogeneous doping concentration of these media and thermal effects linked to their pumping, can ultimately degrade the spatial quality of the beam. This spatial quality can be improved by means of active optics in order to keep the focal spot near the theoretical limit determined by diffraction.

Speaking about spatial quality of a laser beam means taking into account the energy distribution (spatial amplitude) and the wavefront (spatial phase) of the beam. These two variables are coupled during the beam propagation. Thus, the energy distribution and the wavefront in a particular plane of propagation are dependant on the energy distribution and phase in an earlier plane. Knowing the spatial phase and amplitude in a particular plane opens the possibility to calculate (for example by Fresnel transformation) the phase and amplitude in any other plane for a freely propagating laser beam. A modulation on the spatial phase can induce modulations on the amplitude in a nearby plane and vice-versa. On the other hand, for two planes imaged through an optical system, the spatial amplitude and phase distributions are proportional.

The simultaneous control of spatial amplitude and phase has already been studied theoretically<sup>47</sup>. This control necessitates at least two active optics. The first one induces a deformation on the spatial phase, which transform into amplitude deformation, and the second active optic is used near the focusing optics to correct the spatial phase aberration initially present in the laser, and the aberrations induced by the first active optics. We will restrict the following to the control of spatial phase only, not addressing the correction of the spatial amplitude (spatial profile), area defined as beam shaping.

Figure 14 shows a schematic of the laser focusing at the end of a CPA system. Directly after the focusing optics (generally an off-axis parabolic mirror), we speak of the near field, by defining the spatial amplitude  $A_m(x,y)$  and the spatial phase  $\varphi_m(x,y)$  of the pulse. The far field corresponds to the area near focus, and at focus this energy

distribution is described by the function  $A(x_f, y_f)$  which is the 2D Fourier Transform of  $A_m(x, y) \times \exp[i\varphi_m(x, y)]$ .

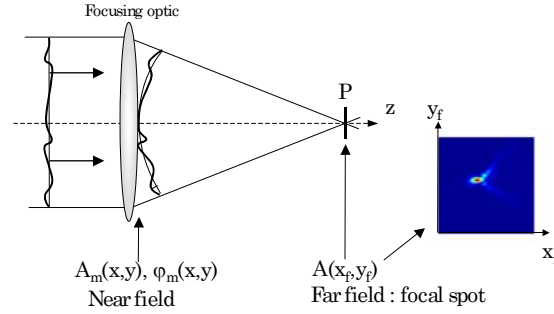


Figure 14 : Principle of laser focusing at end of a laser chain

It is possible to quantify aberrations present in a given wavefront  $\varphi_m(x, y)$  by decomposing them according to their type (Tilt, focus term, astigmatism, coma, ...) and giving the relative amount of each aberration in Peak-to-Valley (PV) or Root Mean Square (RMS) values. For a circular pupil, the set of polynomials called Zernike Polynomials<sup>48</sup> are very useful for that purpose. However, the effect on the focal spot of different aberrations with the same PV value will not decrease the peak intensity by the same amount. The interesting value to know for physical experiments with very high intensity lasers is the peak intensity at the focal point. To characterize the spatial quality of the laser beam, we will then use the Strehl Ratio criterion, defined as follows:

$$SR_\varphi = \frac{\text{Max}\left\{ \left| FT[A_m(x, y) \times \exp(i \cdot \varphi_m(x, y))] \right|^2 \right\}}{\text{Max}\left\{ \left| FT[A_{\text{ref}}(x, y)] \right|^2 \right\}} \quad (18)$$

FT is the 2D Fourier transform operation and  $A_m(x, y)$  and  $\varphi_m(x, y)$  are the measured amplitude and spatial phase in the plane of the focusing optic (cf. Figure ). The classical definition of the Strehl Ratio (used initially in astronomy to quantify the quality of images degraded by atmospheric turbulence) uses a flat amplitude and phase for the reference beam (denominator). It is more appropriate for a CPA laser to use as a reference profile,  $A_{\text{ref}}(x, y)$ , a Gaussian spatial profile or the measured profile itself<sup>49</sup>. In that case, we have a criterion that quantifies the quality of the spatial phase and not the spatial profile; this is why we used the notation  $SR_\varphi$ . When no aberrations are present in the wavefront, the Strehl ratio is equal to 1.

Different techniques have been developed to measure the wave front aberrations of a laser beam, to cite only a few: Shack-Hartmann Wavefront Sensor (SHWS)<sup>50</sup>, a three-wave lateral shearing interferometer<sup>51</sup>, use of a birefringent crystal<sup>52</sup> or the measurement of spatial profile in 3 different planes<sup>53</sup>. Using one opposed to another is a question of resolution of the bi-dimensional measured phase, speed of measurement, ease of use and

cost. Typically, the most common one, the SHWS (cf. Figure ), will give from 32x32 to 128x128 points of measurement on a beam.

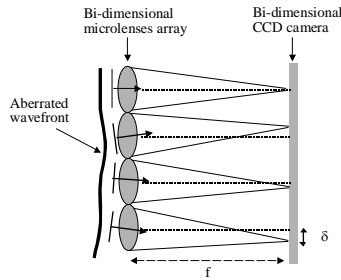


Figure 15 : Schematic of a Shack-Hartmann Wavefront Sensor. A 2D microlenses array gives different focuses on a CCD camera. The shift  $\delta$  of each focal position gives access to the local wavefront slope.

After measuring these wavefront aberrations, it is desirable to correct them with active optics. Spatial light modulators and deformable mirrors have been used to correct these wavefront aberrations, deformable mirrors having a higher damage threshold are usually used on high intensity CPA systems. A deformable mirror is a mirror whose surface is changed to obtain the inverse shape of the phase distortions to be corrected. Voltages applied on actuators control the surface shape of the mirror. Figure 13 gives an example of voltage pattern obtained after a wavefront correction with a 37-actuator deformable mirror. The laser beam covers the central part and the smallest ring of actuators; the outer ring is for wavefront continuity purposes.

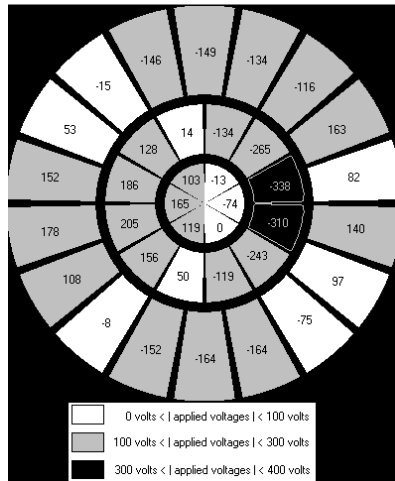


Figure 13: Example of actuator geometry pattern and applied voltages after a wavefront correction (taken from reference<sup>54</sup>)

Wavefront correction is usually accomplished in a closed loop operation. The measurement of the distorted wavefront is sent to the deformable mirror that corrects them. A proper calibration with a matrix inversion procedure allows calculation of the correct voltage to apply to eliminate the wavefront distortion. Figure 14 illustrates this

closed loop operation at the end of a laser system in the case of wavefront correction for a 100 TW laser<sup>55</sup>.

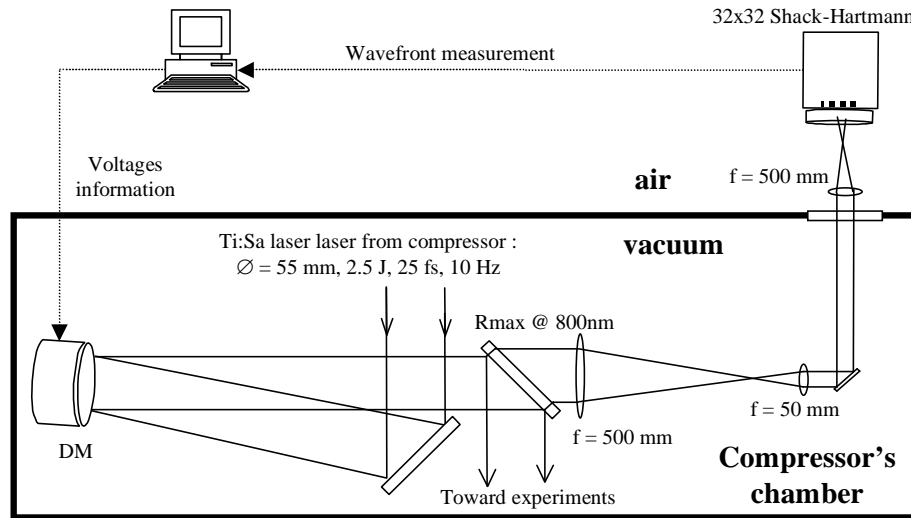


Figure 14: Experimental setup for the wavefront correction on a 100-TW laser. The mirror is under vacuum after the grating compressor and the SHWS is placed outside of vacuum chamber.

In some particular cases, as for the correction of a laser beam focused by a very short focal length parabolic mirror, reliable wavefront measurement is difficult to implement. Optimizations methods based on convergence algorithms (like genetic algorithms) can then be used. The algorithm tests different combinations of the actuator voltages and keep the ones that optimize a convergence criterion. Second harmonic generation in BBO<sup>56</sup> or third harmonic generation on a slide interface<sup>57</sup> are examples of physical criterion that are optimized with these types of convergence loops. The advantages of these methods are that a physical parameter at the focus is really optimized. One of the drawbacks is the time of convergence, which is often several minutes on a kHz laser system, and not applicable to lower repetition rate laser chain (i.e. 10 Hz / 20 Hz systems).

## References

1. Carman, R. L., Benjamin, R. F. & Rhodes, C. K. *Physical Review A* 24, 2649 (1981).
2. Bunkenburg, J. et al. *IEEE Journal of Quantum Electronics* QE-17, 1620 (1981).
3. Luk, T. S., McPherson, A., Gibson, G., Boyer, K. & Rhodes, C. K. *Optics Letters* 14, 1113 (1989).
4. Endoh, A., Watanabe, M., Sarukura, N. & Watanabe, S. *Optics Letters* 14, 353 (1989).
5. Strickland, D. & Mourou, G. Compression of amplified chirped optical pulses. *Opt. Commun.* 56, 219-221 (1985).
6. Maine, P. & Mourou, G. Amplification of 1-nsec pulses in Nd:Glass followed by compression to 1 psec. *Opt. Lett.* 13, 467-469 (1988).
7. Maine, P., Strickland, D., Bado, P., Pessot, M. & Mourou, G. Generation of Ultrahigh Peak Power Pulses by Chirped Pulse Amplification. *IEEE J. Quant. Electron.* 24, 398 (1988).
8. Yamakawa, K., Shiraga, H., Kato, Y. & Barty, C. P. J. Prepulse-free 30-TW, 1-ps Nd:glass laser. *Opt. Lett.* 16, 1593-1595 (1991).
9. Rouyer, C. et al. Generation of 50-TW femtosecond pulses in a Ti:sapphire/Nd:glass chain. *Opt. Lett.* 18, 214-216 (1993).
10. Perry, M., Pennington, P. & Stuart, B. C. *Optics Letters* 24, 160 (1999).
11. Tabak, M., Hammer, J. & Glinsky, M. E. *Physics of Plasmas* 1, 1626 (1994).
12. Schoenlein, R. W. et al. Generation of femtosecond X-ray pulses via laser-electron beam interaction. *Applied Physics B (Lasers and Optics)* B71, 1-10 (2000).
13. Schoenlein, R. W. et al. Femtosecond X-ray pulses at 0.4 Å generated by 90 degrees Thomson scattering: a tool for probing the structural dynamics of materials. *Science* 274, 236-8 (1996).
14. Bula, C., McDonald, K. T. & Prebys, E. J. *Physical Review Letters* 76, 3116 (1996).
15. Telnov, V. I. *Nucl. Instrum. Method A* 294, 72 (1990).
16. Telnov, V. I. *International Journal of Modern Physics A* 15, 2577 (2000).
17. Telnov, V. I. *Nucl. Instrum. Method A* 472, 43 (2001).
18. Yokoya, K. *NIMPR A* 455 (2000).
19. Migus, A., Shank, C. V., Ippen, E. P. & Fork, R. L. *IEEE Journal of Quantum Electronics* QE18, 101 (1982).
20. Treacy, E. B. Optical Pulse Compression With Diffraction Gratings. *IEEE J. Quant. Electron.* QE-5, 454-8 (1969).
21. Martinez, O. E. 3000 times grating compressor with positive group velocity dispersion: application to fiber compensation in 1.3-1.6 μm region. *IEEE J. Quantum Electron.* QE-23, 59-64 (1987).
22. Pessot, M., Maine, P. & Mourou, G. 1000 times expansion/compression of optical pulses for chirped pulse amplification. *Opt. Commun.* 62, 419-21 (1987).

23. Pessot, M., Squier, J., Bado, P., Mourou, G. & Harter, D. J. Chirped Pulse Amplification of 300 fs Pulses in an Alexandrite Regenerative Amplifier. *IEEE J. Quantum Electron.* 25, 61-6 (1988).
24. Frantz, L. M. & Nodvick, J. S. Theory of pulse propagation in a laser amplifier. *Journal of Applied Physics* 34, 2346-2444 (1963).
25. Du, D. et al. Terawatt Ti:sapphire laser with a spherical reflective-optic pulse expander. *Optics Letters* 20, 2114 (1995).
26. Cheriaux, G. et al. Aberration-free stretcher design for ultrashort-pulse amplification. *Optics Letters* 21, 414-416 (1996).
27. Lemoff, B. E. & Barty, C. P. J. Quintic-phase-limited, spatially uniform expansion and recompression of ultrashort optical pulses. *Opt. Lett.* 18, 1651-1653 (1993).
28. Walker, B. C. et al. A 50-EW/cm<sup>2</sup> Ti:sapphire laser system for studying relativistic light-matter interactions. *Optics Express* 5, 196-202 (1999).
29. Kane, S. & Squier, J. Fourth-order-dispersion limitations of aberration-free chirped-pulse amplification systems. *Journal of the Optical Society of America B* 14, 1237 (1997).
30. Squier, J., Barty, C. P. J., Salin, F., Le Blanc, C. & Kane, S. Use of mismatched grating pairs in chirped-pulse amplification systems. *Applied Optics* 37, 1638-41 (1998).
31. Kane, S. & Squier, J. Grating compensation of third-order material dispersion in the normal dispersion regime: Sub-100-fs chirped-pulse amplification using a fiber stretcher and grating-pair compressor. *IEEE J. Quantum Electron.* 31, 2052-2057 (1995).
32. Kane, S. & Squier, J. in *Generation, Amplification, and Measurement of Ultrashort Laser Pulses II* (eds. Wise, F. W. & Barty, C. P. J.) 330 (SPIE, Bellingham, WA, 1995).
33. Gibson, E. et al. Efficient reflection gratings for pulse compression and dispersion compensation of femtosecond pulses. *Optics Letters* 31, 3363-3365 (2006).
34. Gaudiosi, D. et al. Multi-kilohertz repetition rate Ti:sapphire amplifier based on down-chirped pulse amplification. *Optics Express* 14, 9277-9283 (2006).
35. Albrecht, G. F., Eggleston, J. M. & Ewing, J. J. Measurements of Ti<sup>3+</sup>:Al<sub>2</sub>O<sub>3</sub> as a lasing material. *Optics Communications* 52, 401 (1985).
36. Moulton, P. F. Spectroscopic and laser characteristics of Ti:Al<sub>2</sub>O<sub>3</sub>. *J. Opt. Soc. Am. B* 3, 125-33 (1986).
37. Lowdermilk, W. H. & Murray, J. E. The multipass amplifier: Theory and numerical analysis. *Journal of Applied Physics* 51, 2436 (1980).
38. Rudd, J. V. et al. Chirped-pulse amplification of 55-fs pulses at a 1-kHz repetition rate in a Ti:Al<sub>2</sub>O<sub>3</sub> regenerative amplifier. *Opt. Lett.* 18, 2044-2046 (1993).
39. Planchon, T. A., Burgy, F., Rousseau, J. P. & Chamberet, J. P. 3D Modeling of amplification processes in CPA laser amplifiers. *Applied Physics B (Lasers and Optics)* 80 (2005).
40. Eggleston, J. M., DeShazer, L. G. & Kangas, K. W. Characteristics and kinetics of laser-pumped Ti:sapphire oscillators. *IEEE Journal of Quantum Electronics* 24, 1009 (1988).

41. Moulton, P. F. Spectroscopic and laser characteristics of Ti:Al<sub>2</sub>O<sub>3</sub>. *Journal of the Optical Society of America B* 3, 125-33 (1986).
42. Yamakawa, K. & Barty, C. Two-color chirped-pulse amplification in an ultrabroadband Ti : sapphire ring regenerative amplifier. *Opt. Lett.* 28, 2402-2404 (2003).
43. Barty, C. P. J. et al. Generation of 18-fs multiterawatt pulses by regenerative pulse shaping and chirped-pulse amplification. *Opt. Lett.* 21, 668-670 (1996).
44. Barty, C. P. J. et al. Regenerative pulse shaping and amplification of ultrabroadband optical pulses. *Opt. Lett.* 21, 219-221 (1996).
45. Koechner, W. *Solid-State Laser Engineering*. Springer Series in Optical Sciences (2006).
46. Salin, F., Le Blanc, C., Squier, J. & Barty, C. Thermal eigenmode amplifiers for diffraction-limited amplification of ultrashort pulses. *Optics Letters* 23, 718 (1998).
47. Wang, K. Y., Qi, Y. & Sun, J. W. Optical-field correction with deformable mirrors. *Journal of the Optical Society of America B* 11, 1674-1679 (1994).
48. Wang, K. Y. & Silva, D. E. Wave-front interpretation with Zernike polynomials. *Applied Optics* 19, 1510-1518 (1980).
49. Ranc, S., Chériaux, G., Ferré, S., Rousseau, J. P. & Chamberet, J. P. Importance of spatial quality of intense femtosecond pulses. *Applied Physics B (Lasers and Optics)* 70, S181-S187 (2000).
50. Southwell, W. H. Wave front estimation from wave front slope measurements. *Journal of the Optical Society of America B* 70 (1980).
51. Primot, J. Three-wave lateral shearing interferometer. *Applied Optics* 32, 6242 (1993).
52. Buse, K. & Luennemann, M. 3D imaging: Wave front sensing utilizing a birefringent crystal. *Physical Review Letters* 85, 3385-3387 (2000).
53. Bruel, L. Numerical phase retrieval from beam intensity measurements in three planes. *Proceedings of SPIE*, 4932 (Laser-Induced Damage in Optical Materials), 590-598 (2002).
54. Planchon, T. A., Mercère, P., Chériaux, G. & Chamberet, J. P. Off axis aberration compensation of focusing with spherical mirrors using deformable mirrors. *Optics Communications* 216, 23 (2003).
55. Planchon, T. A., Rousseau, J. P., Burgy, F., Chériaux, G. & Chamberet, J. P. Adaptive wavefront correction on a 100-TW / 10 Hz chirped pulse amplification laser and effect of residual wavefront on beam propagation. *Optics Communications* 252, 222-228 (2005).
56. Albert, O., Wang, H., Liu, D., Chang, Z. & Mourou, G. Generation of relativistic intensity pulses at kilohertz repetition rate. *Optics Letters* 25, 1125 (2000).
57. Planchon, T. A. et al. Adaptive correction of a tightly focused, high-intensity laser beam by use of a third harmonic signal generated at an interface. *Optics Letters* 31, 2214 (2006).